ELSEVIER

Probabilistic Engineering Mechanics 17 (2002) 201–213

PROBABILISTIC ENGINEERING MECHANICS

www.elsevier.com/locate/probengmech

Advanced analysis of coupled buffeting response of bridges: a complex modal decomposition approach

Xinzhong Chen*, Ahsan Kareem

Department of Civil Engineering and Geological Sciences, University of Notre Dame, 163 Fitzpatrick, Notre Dame, IN 46556-0767, USA

Received 15 May 2001; accepted 4 January 2002

Abstract

This paper presents a framework based on a complex modal decomposition technique for predicting coupled buffeting response of bridges in both time and frequency domains. The coupled equations of motion in structural modal coordinates with frequency dependent aeroelastic self-excited terms are approximated by frequency independent state-space equations, without augmented aerodynamic states, which retain the complex modal properties of the original system. These equations are then decomposed into a set of uncoupled equations of motion for buffeting response analysis. The frequency dependent unsteady buffeting characteristics and their spanwise correlation are considered in both frequency and time domain analyses instead of invoking the customary quasi-steady assumption. This framework significantly enhances computational efficiency in the frequency domain analysis by avoiding system matrix inversion at each discretized frequency when evaluating the transfer function matrix. Furthermore, it also offers simulation of buffeting response in the time domain that includes frequency dependence of buffeting and self-excited forces. A detailed discussion concerning the complex modal frequencies, damping ratios, mode shapes, and the significance of structural modes on the multimode coupled buffeting response is provided. This helps to glean additional insight and to improve our understanding of the underlying physics of wind–structure interactions. Examples of long span suspension bridges are provided to illustrate the proposed scheme and to demonstrate its effectiveness.

Keywords: Flutter; Buffeting; Complex modal analysis; Bridges; Wind; Random vibration

1. Introduction

With the increase in span length of bridges, natural frequencies and the ratio between the fundamental frequencies in the torsional and vertical modes have decreased significantly. This leads to increased coupling between the vertical and torsional motions under strong winds. As a result, analysis of buffeting and flutter response of long span bridges generally requires consideration of multimodal response and aerodynamic coupling [1–4].

Aerodynamic forces on bridges are conventionally separated into buffeting and self-excited force components. While the buffeting forces due to wind fluctuations are forced excitations, the self-excited forces due to bridge motion alter the stiffness and damping characteristics of the bridge. These modifications are frequency dependent since they depend on the aeroelastic parameters, i.e. flutter derivatives which are functions of reduced frequency or reduced velocity. As a consequence of the self-excited forces, the frequencies, damping ratios and the mode shapes change with an increase in wind velocity. Particularly, the coupled self-excited forces modify the mode shapes that change from real-valued to complex-valued. At a given wind velocity, this complex modal information can be calculated using an iterative calculation procedure. Alternatively, frequency independent state-space equations of motion with augmented aerodynamic states can be utilized to avoid iterative calculations with enhanced computational efficiency [3,5]. This integrated state-space formulation can be realized through the rational function approximation of self-excited forces [6–9].

Buffeting response prediction has been conventionally conducted in the frequency domain using spectral analysis approaches. This is mainly due to the fact that the wind loading parameters are functions of frequency, and the frequency domain provides a convenient format for linear analysis. However, the time domain approach is most appropriate if the analysis involves structural and/or aerodynamic nonlinearities. Chen et al. [4] proposed a time domain approach that incorporates the frequency dependent unsteady aerodynamic force features rather than assumes

* Corresponding author. Tel.: +1-574-631-6648; fax: +1-574-631-9236.
E-mail address: xchen@nd.edu (X. Chen).

0266-8920/02/$ - see front matter
PII: S0266-8920(02)00005-X

frequency independence by invoking the quasi-steady theory used in most previous time domain studies. Recently, Chen and Kareem [10] presented a computationally more efficient framework using a state-space model of the integrated loading and structural system with a vector-valued white noise input. This approach integrates the mathematical representation of multi-correlated wind fluctuations, unsteady buffeting and self-excited forces and the bridge dynamics. The state-space framework facilitates a direct evaluation of the response covariance as well as the time domain simulation of bridge loading and response, and offers a convenient formulation readily amenable to the design of motion control devices.

For linear structures with linear self-excited forces, the buffeting analysis can be conducted based on complex modal analysis, in which the effects of self-excited forces are included in terms of the complex mode information [5,11,15]. Cremona and Solares [11] proposed a simplified approach that avoids inversion of the system matrix at each discretized frequency when evaluating the transfer function matrix. This is based on the assumption that the modal frequencies are well separated for lightly damped structures. In Ref. [15], the complex modes were calculated directly based on a three-dimensional finite element model of the bridge, and the generalized buffeting forces associated with the complex modes were used in the frequency domain spectral analyses. They also conducted a time domain analysis using quasi-steady buffeting forces. In Ref. [5], the equations of structural motion were expressed in terms of frequency independent state-space equations of the integrated system of bridge and associated aerodynamics. The modal description of both the structure and the augmented aerodynamic states were used in the calculation of the transfer function matrix which avoids inversion of a system matrix at each discretized frequency.

In this paper, a framework for predicting coupled buffeting response of bridges in both frequency and time domains is presented based on a complex modal decomposition technique. The frequency dependent coupled equations of bridge motion with aeroelastic self-excited terms are described first in terms of structural modal coordinates. These are then approximated by frequency independent state-space equations without augmented aerodynamic states, which are subsequently decomposed into a set of uncoupled equations for buffeting analysis. The complex modal analysis in the reduced structural modal space offers better physical insight into the aerodynamic coupling among structural modes due to the self-excited forces. This scheme is computationally more efficient than that based on the equations of the bridge motion in physical coordinates. The frequency dependent buffeting and self-excited force characteristics, and their spanwise correlation are considered in both frequency and time domain analyses. The role of complex modal frequencies, damping ratios, mode shapes, and the significance of natural modes on the multimode coupled response is discussed in detail, which helps to glean additional insight and to improve our understanding of the underlying physics of wind–structure interactions. Examples of long span suspension bridges are used to illustrate the proposed scheme and to demonstrate its effectiveness.

2. Theoretical background

This section describes the equations of motion and their state-space representation. Utilizing this formulation, both time and frequency domain analyses are outlined.

2.1. Equations of motion

The equations of motion of an N degree-of-freedom bridge in terms of first M ($M < N$) structural modal coordinates $\mathbf{q}$ are expressed as

$$\mathbf{M}\ddot{\mathbf{q}} + \mathbf{C}\dot{\mathbf{q}} + \mathbf{K}\mathbf{q} = \mathbf{Q}_{\mathrm{se}} + \mathbf{Q}_{\mathrm{b}} \tag{1}$$

where $\mathbf{M} = \mathrm{diag}[m_j]$, $\mathbf{C} = \mathrm{diag}[2\xi_{sj}\omega_{sj}m_j]$ and $\mathbf{K} = \mathrm{diag}[2\xi_{sj}\omega_{sj}m_j]$ are $M \times M$ generalized mass, damping and stiffness matrices, respectively; m_j, ξ_{sj}, and ω_{sj} are the generalized mass, damping coefficient and circular frequency for jth structural mode; $\mathbf{Q}_{\mathrm{se}}$ and $\mathbf{Q}_{\mathrm{b}}$ are $M \times 1$ generalized self-excited and buffeting force vectors, respectively.

The generalized self-excited and buffeting forces can be expressed as

$$\mathbf{Q}_{\mathrm{se}} = \frac{1}{2}\rho U^2\left(\mathbf{A}_{\mathrm{s}}\mathbf{q} + \frac{b}{U}\mathbf{A}_{\mathrm{d}}\dot{\mathbf{q}}\right) \tag{2}$$

$$\mathbf{Q}_{\mathrm{b}} = \frac{1}{2}\rho U^2\left(\mathbf{A}_{\mathrm{b}u}\frac{\mathbf{u}}{U} + \mathbf{A}_{\mathrm{b}w}\frac{\mathbf{w}}{U}\right) \tag{3}$$

where ρ is the air density; U is the mean wind velocity; $\mathbf{A}_{\mathrm{s}}$ and $\mathbf{A}_{\mathrm{d}}$ are the aerodynamic stiffness and damping matrices, respectively, which are functions of flutter derivatives and structural mode shapes [2,4,12]; $\mathbf{A}_{\mathrm{b}u}$ and $\mathbf{A}_{\mathrm{b}w}$ are the buffeting force matrices, which are functions of admittance and joint acceptance functions and structural mode shapes [3,13]; and $\mathbf{u}$ and $\mathbf{w}$ are the fluctuating wind vectors at element nodes for the longitudinal u and vertical w components, respectively. Accordingly, the equations of structural motion are expressed in the state-space format as

$$\dot{\mathbf{Y}}_0 = \mathbf{A}_0\mathbf{Y}_0 + \mathbf{B}_0\mathbf{Q}_{\mathrm{b}} \tag{4}$$

where

$$\mathbf{Y}_0 = \begin{Bmatrix} \mathbf{q} \\ \dot{\mathbf{q}} \end{Bmatrix}; \qquad \mathbf{A}_0 = \begin{bmatrix} \mathbf{0} & \mathbf{I} \\ -\mathbf{M}^{-1}\mathbf{K}_1 & -\mathbf{M}^{-1}\mathbf{C}_1 \end{bmatrix}; \qquad \mathbf{B}_0 = \begin{Bmatrix} \mathbf{0} \\ \mathbf{M}^{-1} \end{Bmatrix} \tag{5}$$

$$\mathbf{C}_1 = \mathbf{C} - \frac{1}{2}\rho U b\mathbf{A}_{\mathrm{d}}(k); \qquad \mathbf{K}_1 = \mathbf{K} - \frac{1}{2}\rho U^2\mathbf{A}_{\mathrm{s}}(k) \tag{6}$$

$k = \omega \frac{b}{v}$ is the reduced frequency; $B = 2b$ is the bridge deck width ω is circular frequency of vibration. It should be noted that the damping and stiffness matrices of the bridge including aeroelastic effects, i.e. $\mathbf{C}_1$, $\mathbf{K}_1$, are frequency dependent and no longer diagonal due to the presence of the coupled aerodynamic damping and stiffness terms.

At a given wind velocity, the eigenvalue λ_j and eigenvector $\mathbf{\Phi}_j$ with their complex conjugates λ_{j+M} and $\mathbf{\Phi}_{j+M}$ ($j = 1,2,\ldots,M$) of the bridge with aeroelastic effects can be evaluated by solving the complex eigenvalue problem

$$\lambda_j \begin{Bmatrix} \mathbf{\Phi}_j \\ \lambda_j \mathbf{\Phi}_j \end{Bmatrix} = \mathbf{A}_0 \begin{Bmatrix} \mathbf{\Phi}_j \\ \lambda_j \mathbf{\Phi}_j \end{Bmatrix} \tag{7}$$

$$\lambda_j = -\xi_j \omega_j + \mathrm{i}\omega_{Dj}; \qquad \omega_{Dj} = \omega_j \sqrt{1 - \xi_j^2} \tag{8}$$

where ω_j and ξ_j are the frequency and damping ratio in jth complex mode; and $\mathrm{i} = \sqrt{-1}$. Since the system matrix $\mathbf{A}_0$ is frequency dependent, an iterative calculation of each eigenvalue is required until the assumed frequency used to evaluate the self-excited forces agrees with the imaginary part of the eigenvalue.

The free vibration associated with the jth complex mode and its complex conjugate counterpart, i.e. $(j+M)$th mode in terms of physical coordinates of the bridge, $\mathbf{Z} = \mathbf{\Psi q}$, is in the form:

$$\begin{aligned} \mathbf{Z}_j(t) &= \mathbf{\Psi}(A_j \mathbf{\Phi}_j \, \mathrm{e}^{\lambda_j t} + A_j^* \mathbf{\Phi}_j^* \, \mathrm{e}^{\lambda_j^* t}) \\ &= 2|A_j||\mathbf{\Psi\Phi}_j| \mathrm{e}^{-\xi_j \omega_j t} \cos(\omega_{Dj} t + \boldsymbol{\varphi}_j + \boldsymbol{\beta}_j) \end{aligned} \tag{9}$$

where $\mathbf{\Psi}$ is $N \times M$ structural mode shape matrix; $\boldsymbol{\varphi}_j$ and $\boldsymbol{\beta}_j$ are the phase angles associated with the vector $\mathbf{\Psi\Phi}_j$ and the scalar A_j, respectively; and A_j depends on the initial conditions. It is important to note that the complex modes retain phase lags between different components of motion, whereas the real-valued natural modes by definition have zero phase lag.

The transfer function matrix between the modal response $\mathbf{q}$ and modal buffeting force $\mathbf{Q}_\mathrm{b}$ is given as

$$\mathbf{H}_\mathbf{q}(\omega) = (-\omega^2 \mathbf{M} + \mathrm{i}\omega \mathbf{C}_1(k) + \mathbf{K}_1(k))^{-1} \tag{10}$$

Conventional coupled buffeting analysis is based on the evaluation of $\mathbf{H}_\mathbf{q}(\omega)$, which requires matrix inversion at each discrete frequency which places a high demand on computational effort. Such a time consuming procedure can be eliminated by using a frequency independent state-space equations of an integrated system of the bridge and aerodynamics. This can be derived by utilizing rational function approximations of the self-excited forces and introducing augmented aerodynamic states [3,5–9].

The self-excited forces corresponding to the steady-state motion $\mathbf{q}(t) = \bar{\mathbf{q}} \, \mathrm{e}^{\mathrm{i}\omega t}$ can be approximated in terms of a rational function:

$$\begin{aligned} \mathbf{Q}_\mathrm{se}(t) &= \frac{1}{2}\rho U^2 (\mathbf{A}_\mathrm{s} + (ik)\mathbf{A}_\mathrm{d})\bar{\mathbf{q}} \, \mathrm{e}^{\mathrm{i}\omega t} \\ &= \frac{1}{2}\rho U^2 \left(\mathbf{A}_1 + (ik)\mathbf{A}_2 + (ik)^2 \mathbf{A}_3 + \sum_{l=1}^{m} \frac{(ik)\mathbf{A}_{l+3}}{ik + d_l} \right) \bar{\mathbf{q}} \, \mathrm{e}^{\mathrm{i}\omega t} \end{aligned} \tag{11}$$

where $\mathbf{A}_1$, $\mathbf{A}_2$, $\mathbf{A}_3$, $\mathbf{A}_{l+3}$ and d_l ($d_l \geq 0$; $l = 1,2,\ldots,m$) are frequency independent matrices and a parameter which can be determined by curve-fitting the experimentally obtained data of $\mathbf{A}_\mathrm{s}(k)$ and $\mathbf{A}_\mathrm{d}(k)$ defined at a set of discretized reduced velocities k_j ($j = 1,2,\ldots$) using a least-square approach.

After some manipulations, the equations of motion can be expressed as the following frequency independent state-space equations:

$$\dot{\hat{\mathbf{Y}}}(t) = \hat{\mathbf{A}}\hat{\mathbf{Y}}(t) + \hat{\mathbf{B}}\mathbf{Q}_\mathrm{b}(t) \tag{12}$$

where

$$\hat{\mathbf{A}} = \begin{bmatrix} \mathbf{0} & \mathbf{I} & \mathbf{0} & \ldots & \mathbf{0} \\ -\bar{\mathbf{M}}^{-1}\bar{\mathbf{K}} & -\bar{\mathbf{M}}^{-1}\bar{\mathbf{C}} & \frac{1}{2}\rho U^2 \bar{\mathbf{M}}^{-1} & \ldots & \frac{1}{2}\rho U^2 \bar{\mathbf{M}}^{-1} \\ \mathbf{0} & \mathbf{A}_4 & -\frac{U}{b} d_1 \mathbf{I} & \ldots & \mathbf{0} \\ \vdots & \vdots & \vdots & \vdots & \\ \mathbf{0} & \mathbf{A}_{3+m} & \mathbf{0} & \ldots & -\frac{U}{b} d_m \mathbf{I} \end{bmatrix};$$

$$\hat{\mathbf{Y}} = \begin{bmatrix} \mathbf{q} \\ \dot{\mathbf{q}} \\ \mathbf{q}_{\mathrm{se}1} \\ \vdots \\ \mathbf{q}_{\mathrm{se}m} \end{bmatrix}; \qquad \hat{\mathbf{B}} = \begin{bmatrix} \mathbf{0} \\ \bar{\mathbf{M}}^{-1} \\ \mathbf{0} \\ \vdots \\ \mathbf{0} \end{bmatrix} \tag{13}$$

where $\bar{\mathbf{M}} = \mathbf{M} - (1/2)\rho b^2 \mathbf{A}_3$, $\bar{\mathbf{C}} = \mathbf{C} - (1/2)\rho U b \mathbf{A}_2$, $\bar{\mathbf{K}} = \mathbf{K} - (1/2)\rho U^2 \mathbf{A}_1$, and $\mathbf{q}_{\mathrm{se}l}$ ($l = 1,2,\ldots,m$) are augmented aerodynamic states.

It is noted that if the self-excited forces can be represented exactly or within an acceptable error by a rational function of the reduced frequency k (Eq. (11)), Eq. (12) completely represents the equations of bridge motion (Eq. (4)) in a frequency independent state space format. Utilizing these frequency independent integrated state-space equations, the flutter analysis can be conducted by solving a linear eigenvalue problem, thus avoiding the iterative procedure needed in the flutter analysis based on frequency dependent state-space equations. This format also facilitates a time domain simulation of the buffeting response and enhances the computational efficiency of frequency domain buffeting analysis by again avoiding the inversion of the system matrix at each discretized frequency [5].

In the present study, a further simplified framework for buffeting response analysis in both time and frequency domains is presented which is based on the complex modal decomposition technique. Assuming that there are no appreciable peaks in the flutter derivatives and the transfer function matrix of the frequency dependent bridge system (Eq. (10)) around the complex modal frequencies can be expressed in terms of the flutter derivatives at the complex modal frequencies, the equations of bridge motion with frequency dependent self-excited forces can then be expressed in the following frequency independent format:

$$\dot{\mathbf{Y}} = \mathbf{A}_{\mathrm{ef}}\mathbf{Y} + \mathbf{B}\mathbf{Q}_{\mathrm{b}} \tag{14}$$

where

$$\mathbf{Y} = \begin{Bmatrix} \mathbf{q} \\ \dot{\mathbf{q}} \end{Bmatrix}; \qquad \mathbf{A}_{\mathrm{ef}} = \begin{bmatrix} \mathbf{0} & \mathbf{I} \\ -\mathbf{M}^{-1}\mathbf{K}_{\mathrm{ef}} & -\mathbf{M}^{-1}\mathbf{C}_{\mathrm{ef}} \end{bmatrix}; \qquad \mathbf{B} = \begin{Bmatrix} \mathbf{0} \\ \mathbf{M}^{-1} \end{Bmatrix} \tag{15}$$

where $\mathbf{K}_{\mathrm{ef}}$, $\mathbf{C}_{\mathrm{ef}}$ are the effective (equivalent) stiffness and damping matrices, which are independent of frequency. For a given wind velocity these can be uniquely determined based on the complex mode information. It is noteworthy that the preceding frequency independent system has the same complex modal properties as the original frequency dependent system.

The equations of the linear system in Eq. (14) can be used for the buffeting response analysis instead of using the frequency dependent state-space formulations (Eq. (4)), or using the frequency independent state-space formulations with augmented aerodynamic states (Eq. (12)). By introducing the following transformation

$$\mathbf{Y}(\mathrm{t}) = \mathbf{\Gamma}\mathbf{R}(t) \tag{16}$$

Eq. (14) can be expressed in terms of $2M$ uncoupled equations [14]:

$$\dot{\mathbf{R}}(t) = \mathbf{\Lambda}\mathbf{R}(t) + \mathbf{\Gamma}^{-1}\mathbf{B}\mathbf{Q}_{\mathrm{b}}(t) \tag{17}$$

where

$$\mathbf{\Gamma} = [\,\mathbf{\Gamma}_1 \quad \mathbf{\Gamma}_2 \quad \dots \quad \mathbf{\Gamma}_{2M}\,] = \begin{bmatrix} \mathbf{\Phi} \\ \mathbf{\Lambda\Phi} \end{bmatrix}; \qquad \mathbf{\Phi} = [\,\mathbf{\Phi}_1 \quad \mathbf{\Phi}_2 \quad \dots \quad \mathbf{\Phi}_{2M}\,] \tag{18}$$

$$\mathbf{\Gamma}^{-1}\mathbf{A}_{\mathrm{ef}}\mathbf{\Gamma} = \mathbf{\Lambda} = \mathrm{diag}[\lambda_j] \tag{19}$$

2.2. Frequency domain analysis

Eqs. (16) and (17) can be expressed in the frequency domain through a Fourier transform

$$\mathbf{q}(\omega) = \mathbf{H}_{\mathbf{q}}(\omega)\mathbf{Q}_{\mathrm{b}}(\omega) \tag{20}$$

in which the transfer matrix $\mathbf{H}_{\mathbf{q}}(\omega)$ is

$$\mathbf{H}_{\mathbf{q}}(\omega) = \mathbf{\Phi}(\mathrm{i}\omega\mathbf{I} - \mathbf{\Lambda})^{-1}\mathbf{\Gamma}^{-1}\mathbf{B} = \sum_{j=1}^{M}\left(\frac{\mathbf{\Phi}_j\mathbf{\Theta}_j^T/m_j}{\mathrm{i}\omega - \lambda_j} + \frac{\mathbf{\Phi}_j^*\mathbf{\Theta}_j^{*T}/m_j}{\mathrm{i}\omega - \lambda_j^*}\right) = \sum_{j=1}^{M} H_{j0}(\omega)((\mathrm{i}\omega)\mathbf{E}^j + \mathbf{F}^j) \tag{21}$$

where

$$\mathbf{\Gamma}^{-1} = \begin{bmatrix} \mathbf{V}_{\mathbf{left}} \\ \mathbf{V}_{\mathbf{right}} \end{bmatrix}; \qquad \mathbf{\Theta} = \mathbf{V}_{\mathbf{right}}^{\mathbf{T}} \tag{22}$$

$$\mathbf{E}^j = \mathbf{\Phi}_j\mathbf{\Theta}_j^T + \mathbf{\Phi}_j^*\mathbf{\Theta}_j^{*T}; \quad \mathbf{F}^j = -(\mathbf{\Phi}_j\mathbf{\Theta}_j^T\lambda_j^* + \mathbf{\Phi}_j^*\mathbf{\Theta}_j^{*T}\lambda_j) \tag{23}$$

$$H_{j0}(\omega) = \frac{1}{m_j(\omega_j^2 - \omega^2 + \mathrm{i}2\xi_j\omega_j\omega)} \tag{24}$$

and superscripts $*$ and T denote complex conjugate operation and matrix transpose operation, respectively. It can be easily illustrated that the rows j and $(j + M)$ of $\mathbf{\Gamma}^{-1}$ and $\mathbf{\Theta}^T$ are complex conjugate pairs.

The contribution of jth and $(j + M)$th complex modes to $\mathbf{q}(\omega)$ is given by

$$\mathbf{q}^j(\omega) = H_{j0}(\omega)((\mathrm{i}\omega)\mathbf{E}^j + \mathbf{F}^j)\mathbf{Q}_{\mathrm{b}}(\omega) \tag{25}$$

For the cases in which the complex modes can be approximated by real-valued structural natural modes, for example, the aerodynamic coupling among structural modes is negligible and the aeroelastic effect can be treated in terms of aerodynamic damping, we have

$$\Phi_{jj} = 1; \qquad \Phi_{jl} = 0 \ \ (j \neq l); \qquad \Theta_{jj} = \frac{-\mathrm{i}}{2\omega_{Dj}}; \qquad \Theta_{jl} = 0 \ \ (j \neq l) \tag{26}$$

$$\mathbf{H}_{\mathbf{q}}(\omega) = \mathrm{diag}[H_{j0}(\omega)] \tag{27}$$

In general, the response quantity of interest, v, is a linear combination of the components of the displacement vector $\mathbf{Z} = \mathbf{\Psi}\mathbf{q}(t)$ as

$$v = \mathbf{B}^T\mathbf{Z} = \mathbf{B}^T\mathbf{\Psi}\mathbf{q}(t) = \mathbf{D}^T\mathbf{q}(t) \tag{28}$$

where $\mathbf{B}$ is a $N \times 1$ constant vector; and $\mathbf{D} = \mathbf{\Psi}\mathbf{B}$ is known as the effective modal participation factor.

The power spectral density (PSD) of the responses $\mathbf{q}$ and v are given by

$$\mathbf{S}_{\mathbf{q}}(\omega) = \mathbf{H}_{\mathbf{q}}^*(\omega)\mathbf{S}_{\mathbf{Qb}}(\omega)\mathbf{H}_{\mathbf{q}}(\omega)^T; \qquad S_v(\omega) = \mathbf{D}^T\mathbf{S}_{\mathbf{q}}(\omega)\mathbf{D} \tag{29}$$

The mean square responses are estimated by integrating the PSDs over the frequency range.

2.3. Time domain analysis

The modal response in time domain can be given as

$$\mathbf{q}(t) = \sum_{j=1}^{M} (\mathbf{\Phi}_j R_j(t) + \mathbf{\Phi}_j^* R_j^*(t)) \quad (30)$$

where $R_j(t)$ is the response in the jth complex mode

$$R_j(t) = \frac{1}{m_j}\int_0^t \mathbf{\Theta}_j^T \mathbf{Q}_{\rm b}(\tau) e^{\lambda_j(t-\tau)}\,d\tau = \mathbf{\Theta}_j^T(-\lambda_j^* \mathbf{y}^j(t) + \dot{\mathbf{y}}^j(t)) \quad (31)$$

where $\mathbf{y}^j(t)$ and $\dot{\mathbf{y}}^j(t)$ are given using the well-known Duhamel integrals:

$$\mathbf{y}^j(t) = \frac{1}{m_j\omega_{Dj}}\int_0^t \mathbf{Q}_{\rm b}(\tau)\exp[-\xi_j\omega_j(t-\tau)]\sin\omega_{Dj}(t-\tau)d\tau \quad (32)$$

$$\dot{\mathbf{y}}^j(t) = \frac{1}{m_j}\int_0^t \mathbf{Q}_{\rm b}(\tau)\exp[-\xi_j\omega_j(t-\tau)]\cos\omega_{Dj}(t-\tau)d\tau - \xi_j\omega_j\mathbf{y}^j(t) \quad (33)$$

Accordingly, the buffeting response of interest $v(t)$ is given by Eq. (28).

It is noted that an element of $\mathbf{y}^j(t)$, i.e. $y_l{}^j(t)$, is the displacement of a single degree-of-freedom system with mass m_j, circular frequency ω_j and damping ratio ξ_j subjected to the excitation $Q_{{\rm b}l}(t)$, where $Q_{{\rm b}l}(t)$ is the generalized buffeting force in the lth structural mode. Recalling the cases in which the complex modes can be approximated by the real-valued structural modes, we have $y_l^j(t) = 0$ ($l \neq j$) which helps to simplify these calculations in real-valued structural mode cases.

Based on the finite element analysis framework, the modal buffeting forces are calculated based on the forces acting on each element. The time histories of unsteady buffeting forces associated with given input wind fluctuations cannot be calculated by directly using the formulations defined in the frequency domain which involve frequency dependent admittance and joint acceptance functions [4] unless the unsteady characteristics are neglected with the customary practice of invoking the quasi-steady theory [9]. For arbitrary wind fluctuations, the associated buffeting forces must be calculated using the convolution integral with the aerodynamic impulse response function or using an equivalent state-space model [4,10].

For example, the lift component of the buffeting forces on an element excited by the w component of the wind excitation is given as

$$L_{{\rm b}w}(t) = -\frac{1}{2}\rho U^2 l \int_{-\infty}^{t}\int_{-\infty}^{\tau_2} J_{Lw}(t-\tau_2) I_{Lw}(\tau_2-\tau_1) \times \frac{w(\tau_1)}{U} d\tau_1\, d\tau_2 \quad (34)$$

where l is the element length; J_{Lw} is the inverse Fourier transform of joint acceptance function $\bar{J}_{Lw}$; I_{Lw} is the impulse response function, and is related to the admittance function χ_{Lw} as

$$\bar{I}_{Lw} = 2b(C_L' + C_D)\chi_{Lw} \quad (35)$$

C_L, C_D are the mean static force coefficients; $C_L' = dC_L/d\alpha$ and the over bar represents the inverse Fourier transform.

In the frequency domain, $L_{{\rm b}w}$ is given as

$$L_{{\rm b}w}(t) = -\frac{1}{2}\rho U^2(2b)l(C_L' + C_D)\chi_{Lw}\bar{J}_{Lw}\frac{w(t)}{U} \quad (36)$$

The aerodynamic admittance and acceptance functions can be expressed in terms of rational function approximations [4,10]

$$\chi_{Lw}(k) = A_1^\chi + \sum_{j=1}^{m^\chi}\frac{(ik)A_{j+1}^\chi}{ik + d_j^\chi} \quad (37)$$

$$\bar{J}_{Lw}(k) = A_1^J + \sum_{j=1}^{m^J}\frac{(ik)A_{j+1}^J}{ik + d_j^J} \quad (38)$$

where A_1^χ, A_{j+1}^χ and d_j^χ ($j = 1, 2, \ldots, m^\chi$), and A_1^J, A_{j+1}^J and d_j^J ($j = 1, 2, \ldots, m^J$) are the frequency independent coefficients determined by curve-fitting the experimental data of aerodynamic admittance and joint acceptance functions. Other forms of rational functions can also be used to describe the frequency dependent functions of aerodynamic forces.

Accordingly, $L_{{\rm b}w}(t)$ given in Eq. (34) is replaced by

$$L_{{\rm b}w}(t) = (A_1^J + \sum_{j=1}^{m^J} A_{j+1}^J)L_{{\rm b}w0}(t) - \sum_{j=1}^{m^J}\frac{d_j^J U}{b}\phi_j^J(t) \quad (39)$$

$$\dot{\phi}_j^J(t) = -\frac{d_j^J U}{b}\phi_j^J(t) + A_{j+1}^J L_{{\rm b}w0}(t) \qquad (j = 1, 2, \ldots, m^J) \quad (40)$$

and

$$L_{{\rm b}w0}(t) = -\frac{1}{2}\rho U^2(2b)(C_L' + C_D)l\left((A_1^\chi + \sum_{j=1}^{m^\chi} A_{j+1}^\chi) \times \frac{w(t)}{U} - \sum_{j=1}^{m^\chi}\frac{d_j^\chi U}{b}\phi_j^\chi(t)\right) \quad (41)$$

$$\dot{\phi}_j^\chi(t) = -\frac{d_j^\chi U}{b}\phi_j^\chi(t) + A_{j+1}^\chi\frac{w(t)}{U} \qquad (j = 1, 2, \ldots, m^\chi) \quad (42)$$

where ϕ_j^J ($j = 1, 2, \ldots, m^J$) and ϕ_j^χ ($j = 1, 2, \ldots, m^\chi$) are the augmented variables. Similar expressions for the other buffeting force components can be presented which have been omitted here for the sake of brevity.

A multi-variate auto-regressive (AR) scheme can be utilized for generating the input wind fluctuations with prescribed spectral description for the time domain analysis [4].

3. Illustrative examples

This section presents illustrative examples to discuss the complex modal properties and the significance of structural modes on the multimode coupled response, and to demonstrate the effectiveness of the analysis scheme introduced here.

3.1. Bridge dynamics and aerodynamic force parameters

A suspension bridge with a main span of nearly 2000 m was used as an example. For simplicity and without loss of generality, only the aerodynamic forces acting on the bridge deck were considered. The von Karman spectra were used to describe u and w components of wind fluctuations. The turbulence intensities and integral length scales were assumed to be 10 and 5%, and 80 and 40 m, for u and w components, respectively. The admittance functions used were based on Davenport's formula for drag with a decay factor of 8, and the Sears function for lift and pitching moment. Two different joint acceptance functions were used for the buffeting force components associated with u and w components, respectively. The drag component of the self-excited forces was evaluated based on the quasi-steady theory. The lift and pitching moment components were calculated based on the flutter derivatives derived from the Theodorsen function. The first 15 natural modes with frequencies ranging from 0.03 to 0.2 Hz were considered for describing the dynamic behavior of the bridge.

3.2. Complex mode properties

Figs. 1 and 2 show the changes in the complex modal frequencies and damping ratios with the increasing mean wind velocity. For comparison, results of mode-by-mode analysis without aerodynamic coupling are also presented. It is noted that in the high frequency range aerodynamic

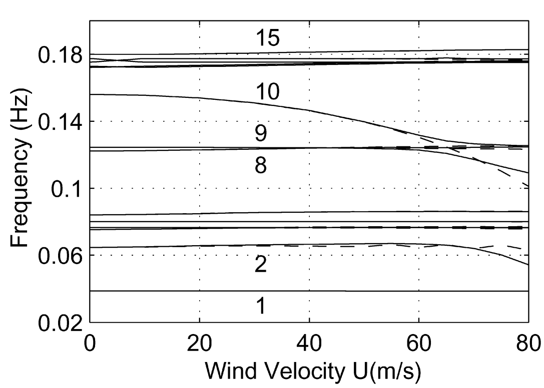

Fig. 1. Complex modal frequency vs. wind velocity (— w/ coupling; – – w/o coupling, mode-by-mode).

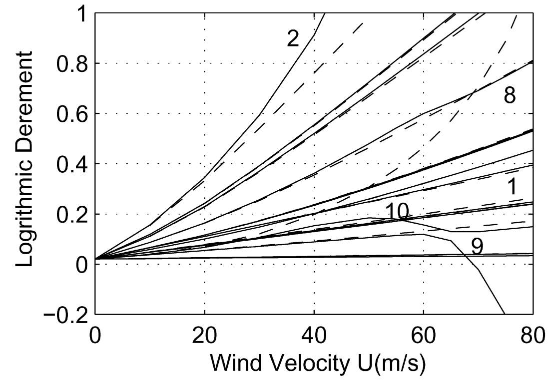

Fig. 2. Complex modal damping vs. wind velocity (— w/ coupling; – – w/o coupling, mode-by-mode).

coupling significantly influences the modal damping. The critical flutter velocity is 68.3 m/s. The mode shapes of some real-valued natural modes (at zero mean velocity) and complex modes at 65 m/s regarding the bridge deck motions in vertical, lateral and torsional directions are presented in Fig. 3. In the case of complex modes, the amplitude ratios and phase lags for the lateral, vertical and torsional motions are presented.

The structural mode 1 represents the first lateral symmetric mode with a slight coupling in the torsional direction. In contrast, the complex mode 1 comprises of a predominant lateral component coupled with vertical and torsional components. Since the coupled aerodynamic forces between lateral and vertical, and between lateral and torsional directions are generally negligible, therefore, these are not included here. Obviously, the presence of vertical and torsional components in the complex mode 1, therefore, results from the aerodynamic coupling between the vertical and torsional directions. Although these coupled components in complex mode 1 are relatively small compared to the modes dominated by the vertical and torsional motions, these may have significant contribution to the overall vertical and torsional buffeting responses, because the response in this complex mode is generally much larger than the higher modes due to its low frequency and associated higher level of wind loading. This coupled response will be clearly illustrated in the response PSD to be discussed later in this paper.

In complex modes 9 and 10, the coupling between the vertical and torsional motions was significant, and the vertical motion was dominated by the first vertical symmetric structural mode (structural mode 2). The second lateral symmetric mode (structural mode 9) also makes a significant contribution to these two complex modes due to its closely spaced frequency at the velocity range of about 65 m/s. Apart from this velocity range, the coupling of structural mode 9 with others is marginal. As shown in Fig. 4, at a wind velocity of 75 m/s, the structural mode 9 dominates the complex mode 10, and the complex mode 9 becomes the vertical and torsional coupled mode. The

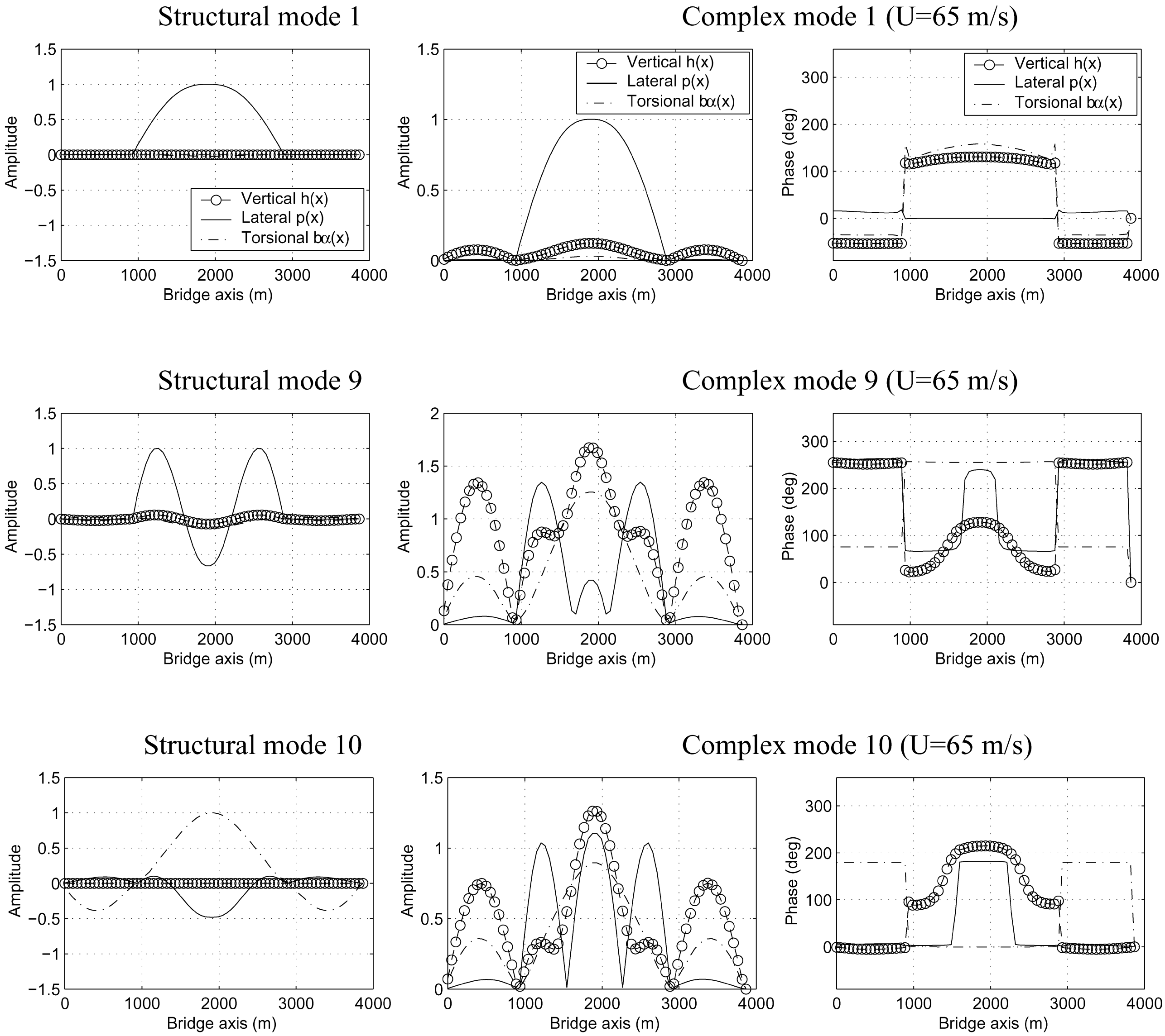

Fig. 3. Mode shapes of the structural modes at $U = 0$ and the complex modes at $U = 65$ m/s (–○– vertical; — lateral; – · – torsional).

modal damping of this coupled complex mode becomes negative and leads to the system becoming unstable beyond the critical flutter velocity. It has been illustrated earlier that the fundamental vertical and torsional modes are the most important modes for coupled flutter of long span suspension bridges [3].

3.3. Frequency domain analysis

In this study, two different calculations were performed for comparison, i.e. (a) fully coupled case in which all uncoupled and coupled aeroelastic terms were included; (b) uncoupled case in which all coupled aeroelastic terms were neglected, i.e. the damping and frequency were evaluated using mode-by-mode approach and the mode shapes were those of real-valued natural structural modes. The frequencies and damping ratios discussed earlier have been shown in Figs. 1 and 2. Fig. 5 shows the PSD of the vertical, lateral and torsional displacements at the quarter and center points of the main span. Fig. 6 shows the root-mean-square (RMS) values of the buffeting response along the bridge axis. From the peak of response PSD at the frequency of the complex mode 1, it is noteworthy that the coupled vertical and torsional components in the complex mode 1 have a significant contribution to the total vertical and torsional responses. As due to its low frequency, an accurate evaluation of this coupling effect requires a reliable estimate of the self-excited forces at very high reduced velocity range. This indicates that the wind velocity range of interest for the measurement of the flutter derivatives should not only satisfy the need of a coupled flutter analysis but it also should provide data pertinent to a coupled buffeting analysis. In this example, at a wind velocity of $U = 65$ m/s, the

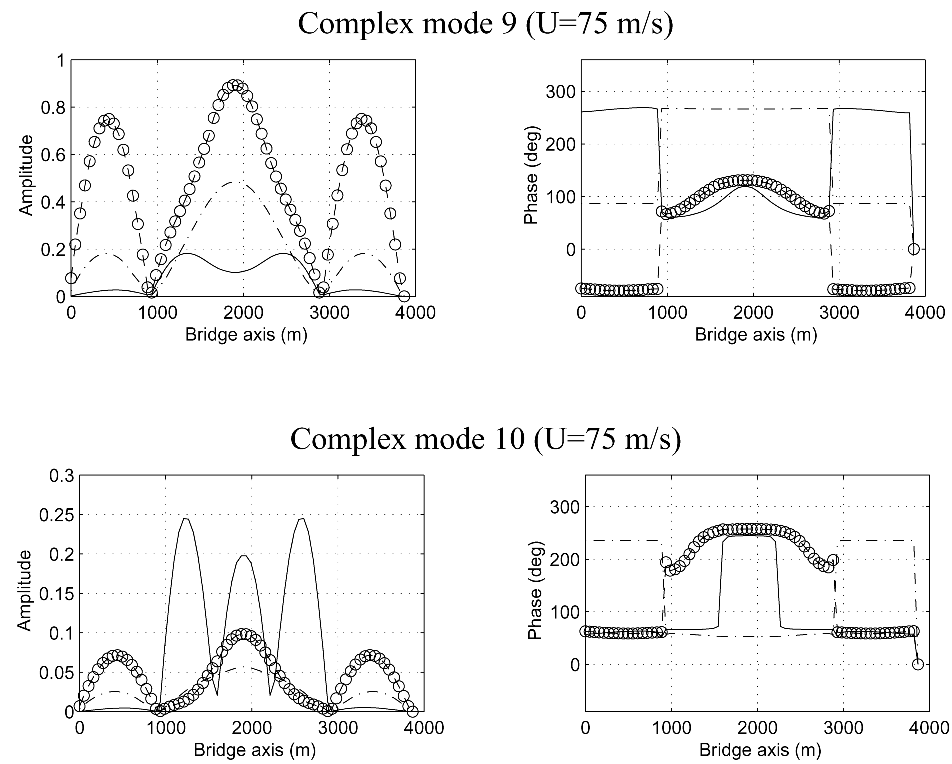

Fig. 4. Complex mode shapes at $U = 75$ m/s (–○– vertical; — lateral; – · – torsional).

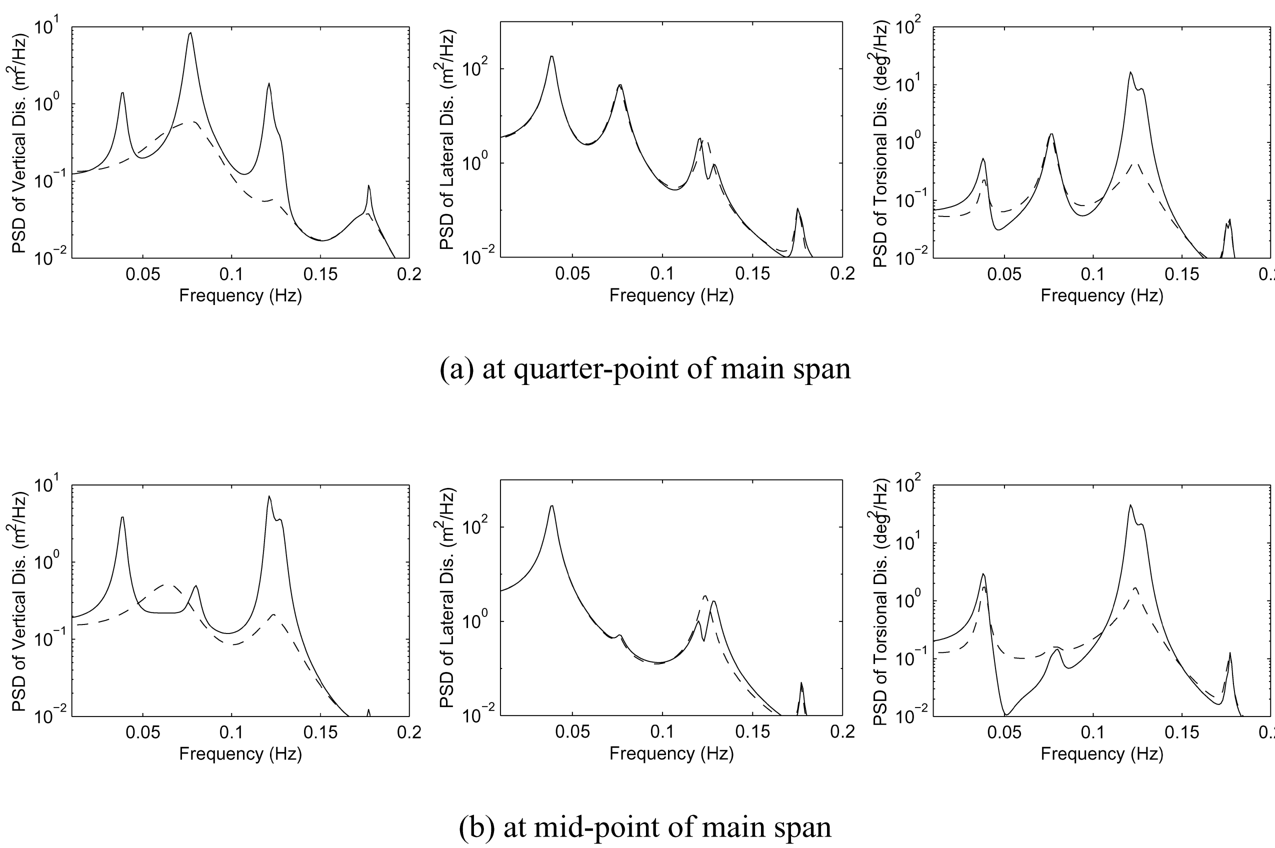

Fig. 5. Power spectra of the buffeting response ($U = 65$ m/s, — w/ coupling; – – w/o coupling).

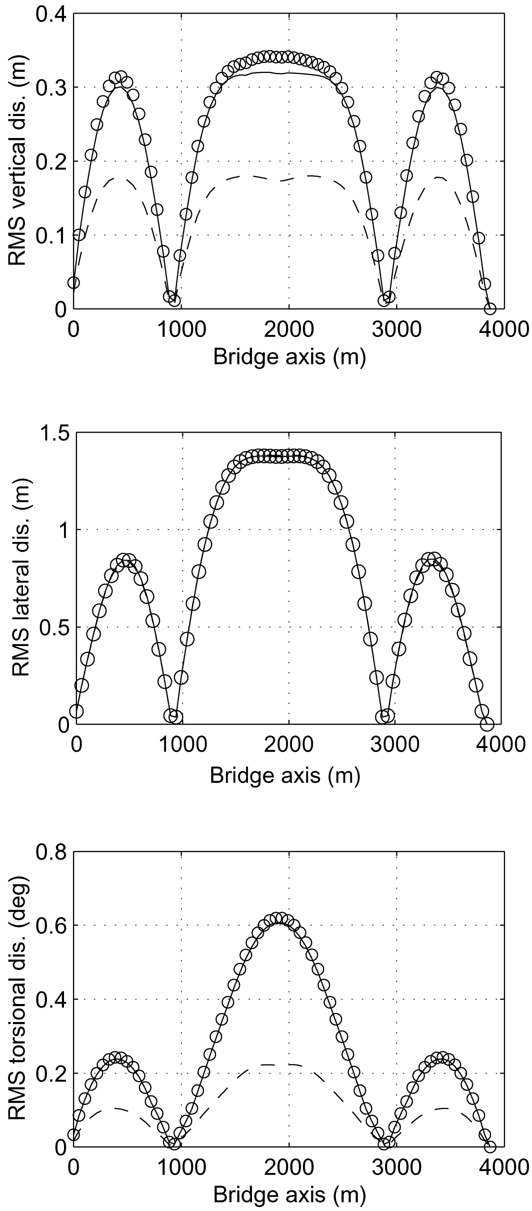

Fig. 6. RMS response ($U = 65$ m/s, — w/ coupling; – – w/o coupling; –○– w/ coupling by conventional analysis).

reduced velocity associated with the first complex mode is $U/(fB) = 47.4$.

The contribution of the complex mode 9 with coupled vertical and torsional motions to the vertical and buffeting response will significantly increase with the increase in the wind velocity near the critical flutter velocity due to the decrease in modal damping. This mode will lead the system to become unstable due to its negative damping beyond the critical flutter velocity. While the lateral response is dominated by the first lateral mode and is little influenced by the aerodynamic coupling, significant differences can be identified in the vertical and torsional responses when neglecting the aerodynamic coupling effects.

The buffeting response based on the transfer function matrix of the frequency dependent bridge system is also presented in Fig. 6 for comparison. Excellent agreement demonstrates the accuracy of the proposed framework based on complex modal decomposition technique.

3.4. Time domain analysis

A time domain analysis was also conducted by simulating time histories of wind fluctuations, unsteady buffeting forces and the corresponding bridge responses. Ten realizations with a total length of 1200 s at a time interval of 0.1 s for each realization were simulated at each mean wind velocity. For each realization the RMS response components were calculated and their mean μ and the standard deviations σ were derived based on the 10 simulated realizations. Fig. 7 shows a set of realizations of the wind fluctuations and buffeting responses at the mid-point of the main span. A comparison of the RMS response with the frequency domain analysis is shown in Fig. 8. For the time domain results, the RMS response is shown in terms of the mean and the 99% confidence intervals $[\mu - 2.58\sigma, \mu + 2.58\sigma]$. An excellent agreement is noted between the time and frequency domain results for the vertical and torsional responses with the exception of some discrepancy in the lateral response. This discrepancy in the lateral response is attributed in part to the accuracy of the PSD representation of the simulated wind fluctuations in the u direction at a very low frequency range.

3.5. Parameter studies

In order to advance our understanding of the aerodynamic coupling among structural modes, a parameter study was conducted by neglecting coupling terms among some of the natural modes while keeping the total number of modes to 15 as considered in the earlier example. Two cases were considered here, first, the aerodynamic coupling terms among only the structural modes 1, 2 and 10, which are the fundamental structural modes in lateral, vertical and torsional directions, respectively, were considered. The second case further included modes 8 and 9, which are the second symmetric vertical mode and the second symmetric lateral mode. The RMS response for these two cases are compared to the fully coupled case and shown in Fig. 9. Results indicate that the structural modes 1, 2, 8, 9 and 10 are most important for describing the coupled buffeting response in strong winds.

To investigate the influence of self-excited forces on the buffeting response, analysis was also carried out by using the flutter derivatives of a twin-box section. Some of the flutter derivatives are shown in Fig. 10 and compared to those derived based on the Theodorsen function. The critical flutter velocity for this example bridge is 73.2 m/s. The PSD and RMS of the buffeting response are presented in Figs. 11 and 12. In this case, the contribution of the first complex mode to the vertical and torsional responses is less important due to the fact that the coupled vertical and torsional

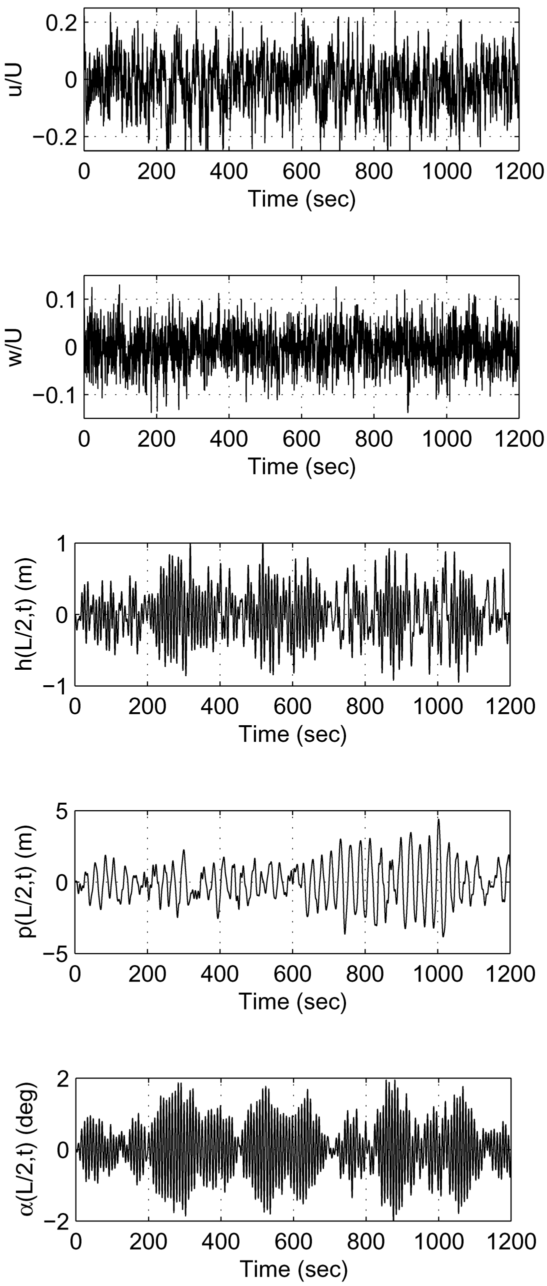

Fig. 7. Realizations of wind fluctuations and buffeting response (mid-point of the main span, $U = 65$ m/s).

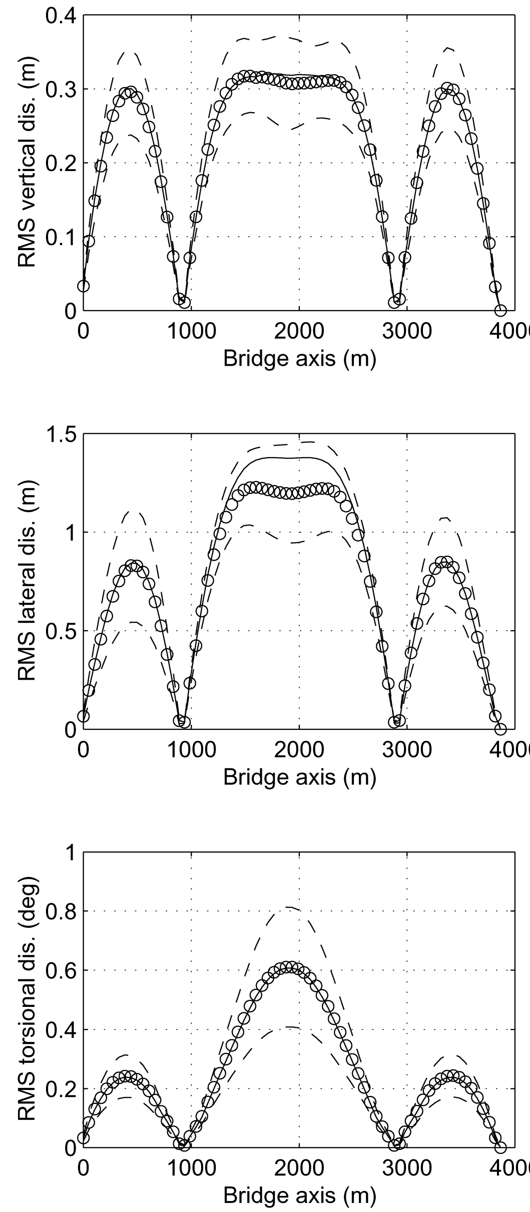

Fig. 8. Comparison of RMS response ($U = 65$ m/s, — frequency domain; –○– mean RMS response from time domain; – – $\mu + 2.58\sigma$ and $\mu - 2.58\sigma$).

motions of this complex mode are comparatively small. Without the aerodynamic coupling, the buffeting response components in vertical and torsional directions are underestimated similar to the previous example. The lateral response of the main span is mainly contributed by the first lateral symmetric mode and is less influenced by aerodynamic coupling, but the responses at the side spans are apparently influenced by the aerodynamic coupling effects. Excellent agreement with the result based on the conventional transfer function matrix of the frequency dependent bridge system illustrated the accuracy of the proposed framework.

4. Concluding remarks

The equations of bridge motion with frequency dependent aeroelastic terms are expressed in terms of simplified frequency independent state-space equations, without augmented aerodynamic states, which retain the original complex modal properties. The simplification is based on the assumptions that there are no appreciable peaks in the flutter derivatives, and the transfer function matrix of the frequency dependent bridge system around the complex modal frequencies can be expressed in terms of the flutter derivatives at the complex modal frequencies. These assumptions are generally satisfied for most bridges. This

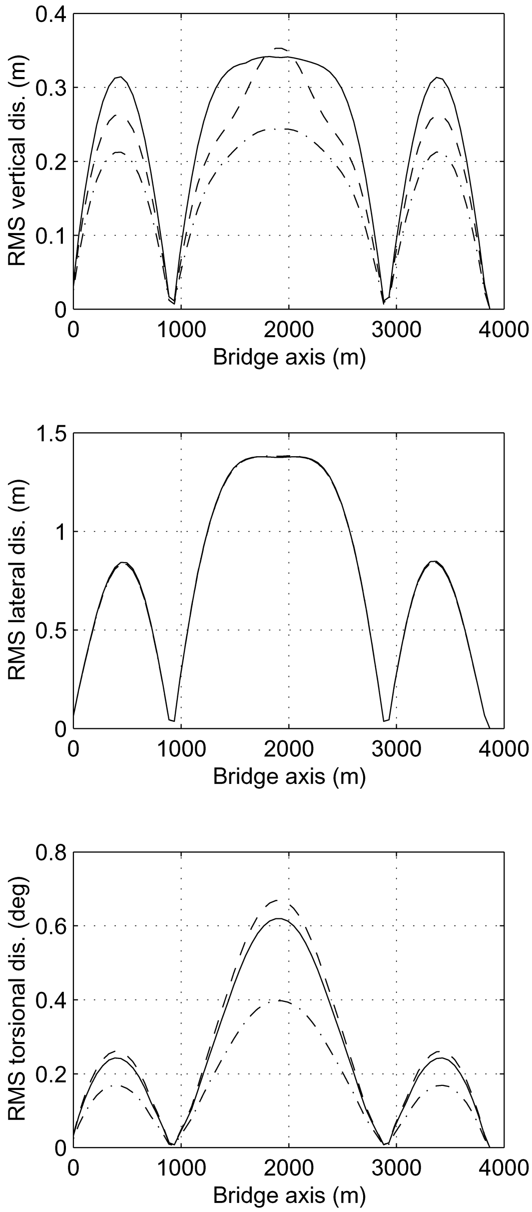

Fig. 9. RMS response ($U = 65$ m/s, — w/ coupling; – – w/ coupling among mode 1, 2, 8–10; – · – w/ coupling among 1, 2, 10).

format enhances computational efficiency in frequency domain analysis by avoiding inversion of the system matrix at each discretized frequency when evaluating the transfer function matrix. This framework also facilitates simulation of the buffeting response in the time domain while still including the frequency dependent characteristics of buffeting and self-excited forces. The complex modal properties of long span bridges due to aeroelastic effects were discussed in detail. This not only provided an enhanced physical insight but also improved our understanding of the aeroelastic behavior of long span bridges under strong winds.

The lateral motion is often coupled with torsional motion due to the structural coupling experienced by most long span suspension bridges. The torsional motion involved in the fundamental lateral natural mode may result in a certain level of coupled vertical motion due to aerodynamic coupling between the vertical and torsional directions. The

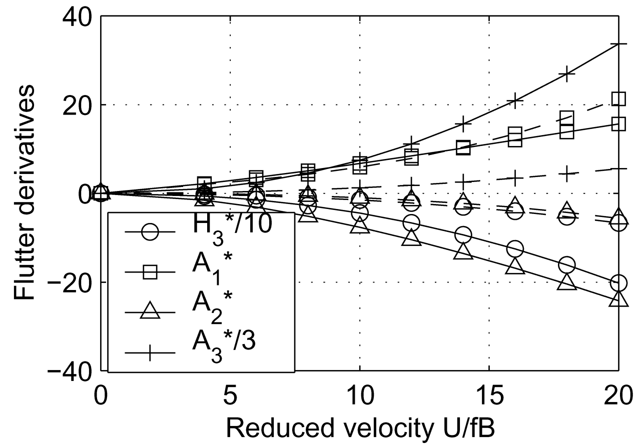

Fig. 10. Flutter derivatives (— given by Theodorsen function; – – for twin-box section).

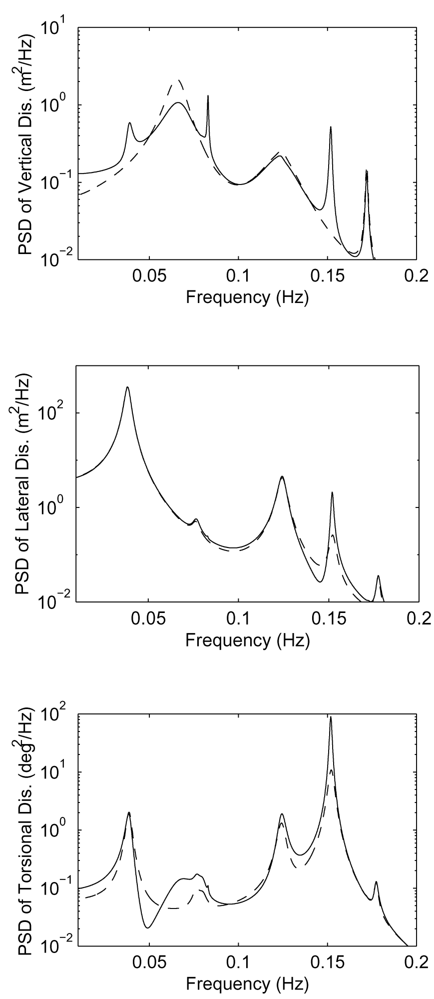

Fig. 11. Power spectra of the buffeting response at mid-point of the main span (twin-box section, $U = 65$ m/s, — w/ coupling; – – w/o coupling).

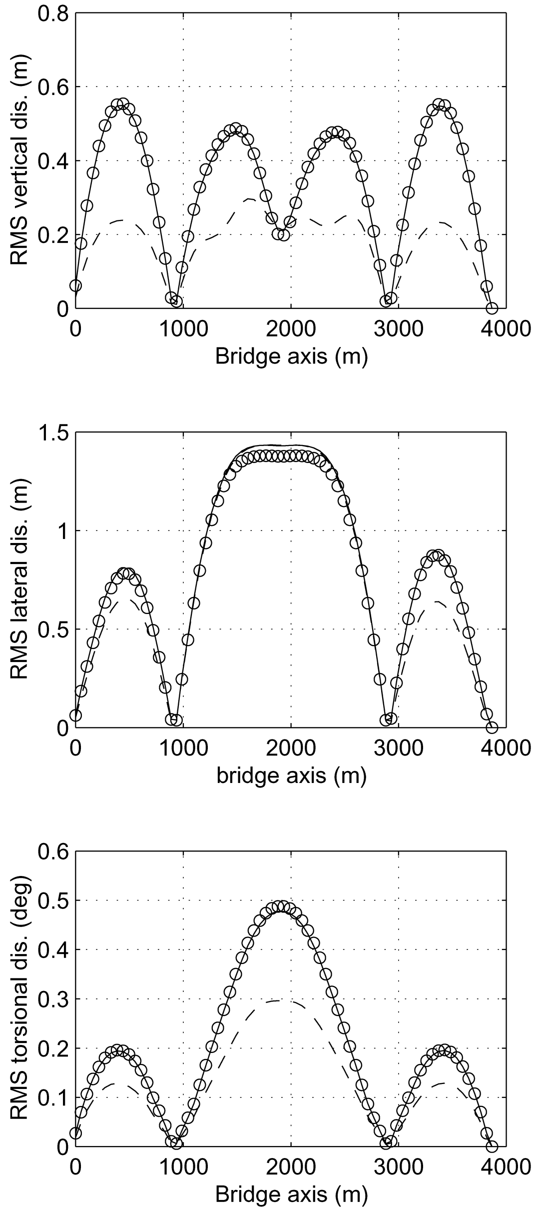

Fig. 12. RMS response (twin-box section, $U = 65$ m/s, — w/ coupling; – – w/o coupling; –○– w/ coupling by conventional analysis).

structural and aerodynamic coupling of motions may make a significant contribution to the total buffeting response in the vertical and torsional directions because of the larger buffeting response of this complex mode which is attributed to its lower frequency and higher wind loading. An accurate evaluation of these coupled motions requires a reliable estimate of the self-excited forces at comparatively higher reduced frequency range than that customarily needed for a coupled multimode flutter analysis.

Aerodynamic coupling results in significantly larger buffeting response in the vertical and torsional directions. It is attributed to the changes in the modal frequencies, and more critically, in the damping ratios and modal shapes. A parameter study indicated that only a few important modes dominate the bridge aeroelastic behavior. A discussion on the significance of the structural natural modes in characterizing the flutter and buffeting responses of long span bridges not only improves our understanding of the physics of wind–bridge interactions, but also provide guidance for the full aeroelastic modeling of bridges in wind tunnel tests, in which the important natural modes must be very accurately modeled.

The time domain simulations that incorporate the simulation of frequency dependent unsteady buffeting and self-excited forces provide a more accurate prediction of response in comparison with customary techniques relying on the quasi-steady formulation. The aerodynamic admittance function and spatial correlation of aerodynamic forces can be accurately considered in the proposed scheme. The time domain analysis presented here also facilitates the consideration of nonlinear buffeting forces and response under non-stationary wind excitations.

Acknowledgements

The support for this work was provided in part by NSF Grants CMS 9402196 and CMS 95-03779. This support is gratefully acknowledged. The writers are thankful to Dr Fred Haan, Jr, visiting assistant professor, Department of Civil Engineering and Geological Sciences, University of Notre Dame, IN, for his comments on the manuscript.

References

[1] Jain A, Jones NP, Scanlan RH. Coupled flutter and buffeting analysis of long-span bridges. J Struct Engng, ASCE 1996;122(7):716–25.
[2] Katsuchi H, Jones NP, Scanlan RH. Multimode coupled flutter and buffeting analysis of the Akashi-Kaikyo Bridge. J Struct Engng, ASCE 1999;125:60–70.
[3] Chen X, Matsumoto M, Kareem A. Aerodynamic coupling effects on flutter and buffeting of bridges. J Engng Mech, ASCE 2000;126(1):17–26.
[4] Chen X, Matsumoto M, Kareem A. Time domain flutter and buffeting response analysis of bridges. J Engng Mech, ASCE 2000;126(1):7–16.
[5] Chen X, Kareem A, Matsumoto M. Multimode coupled flutter and buffeting analysis of long span bridges. J Wind Engng Ind Aerodyn 2001;89(7–8):649–64.
[6] Roger KL. Airplane math modeling methods for active control design. AGARD-CP-228; 1977.
[7] Karpel M. Design for active flutter suppression and gust alleviation using state-space aeroelastic modeling. J Aircraft 1982;19(3):221–7.
[8] Matsumoto M, Chen X, Shiraishi N. Buffeting analysis of long span bridge with aerodynamic coupling. Proceedings of the 13th National Symposium on Wind Engineering, Japan Association for Wind Engineering; 1994. p. 227–32 (in Japanese).
[9] Wilde K, Fujino Y, Masukawa J. Time domain modeling of bridge deck flutter. Struct Mech Earthquake Engng, JSCE 1996;13(2):93–104.
[10] Chen X, Kareem A. Aerodynamic analysis of bridges under multi-correlated winds: integrated state-space approach. J Engng Mech 2001;127(11):1124–34.
[11] Cremona C, Solares AP. Simplified approach for assessing bridge buffeting response with aeroelastic interaction. Proceedings of

Second East European Conference on Wind Engineering, Prague; 1998. p. 89–96.
[12] Scanlan RH. The action of flexible bridges under wind. I. Flutter theory. J Sound Vibr 1978;60(2):187–99.
[13] Scanlan RH. The action of flexible bridges under wind. II. Buffeting theory. J Sound Vibr 1978;60(2):201–11.
[14] Soong TT, Grigoriu M. Random vibration of mechanical and structural systems. Englewood Cliffs, NJ: Prentice-Hall, 1993.
[15] Yamada H, Miyata T, Minh NN, Katsuchi H. Complex flutter-mode analysis for coupled gust response of the Akashi Kaikyo Bridge model. In: Larsen A, Larose TL, Livesey FM, editors. Wind engineering into 21st century. Rotterdam: Balkema, 1999. p. 1081–8.